

Electronic Supporting Information (ESI)

For

Light-triggered CO delivery by a water-soluble and biocompatible manganese photoCORM

Jorge Jimenez, Indranil Chakraborty, Samantha J. Carrington and Pradip K. Mascharak*

*Contribution from the Department of Chemistry and Biochemistry,
University of California Santa Cruz, CA 95064, USA*

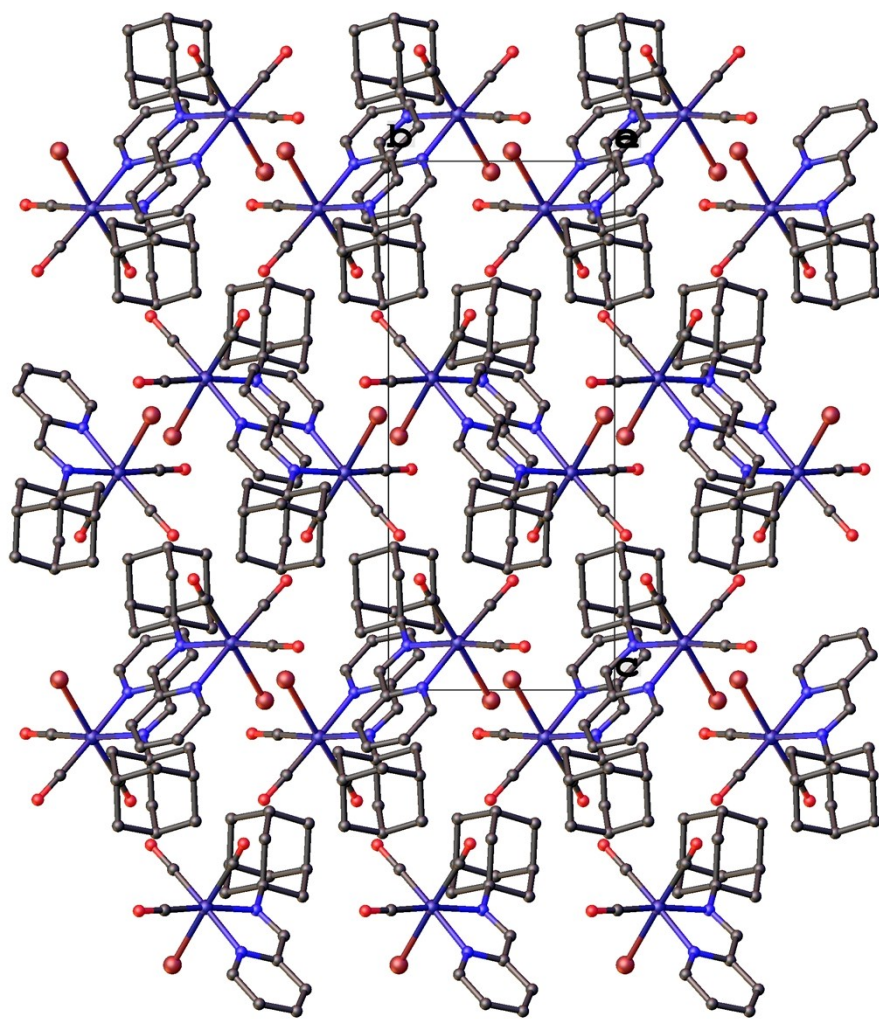


Fig. S1. Packing diagram of **1** along a axis

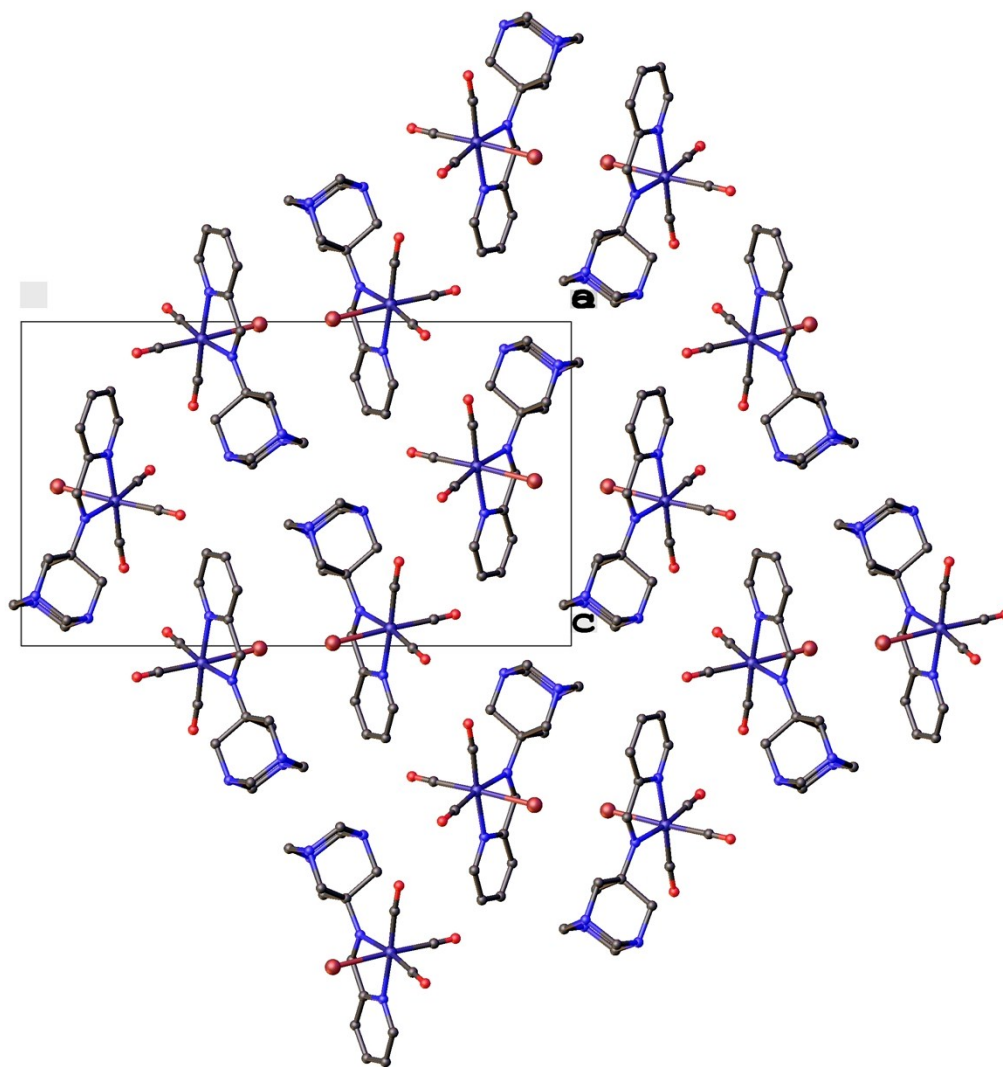


Fig. S2. Packing diagram of **2** along *a* axis

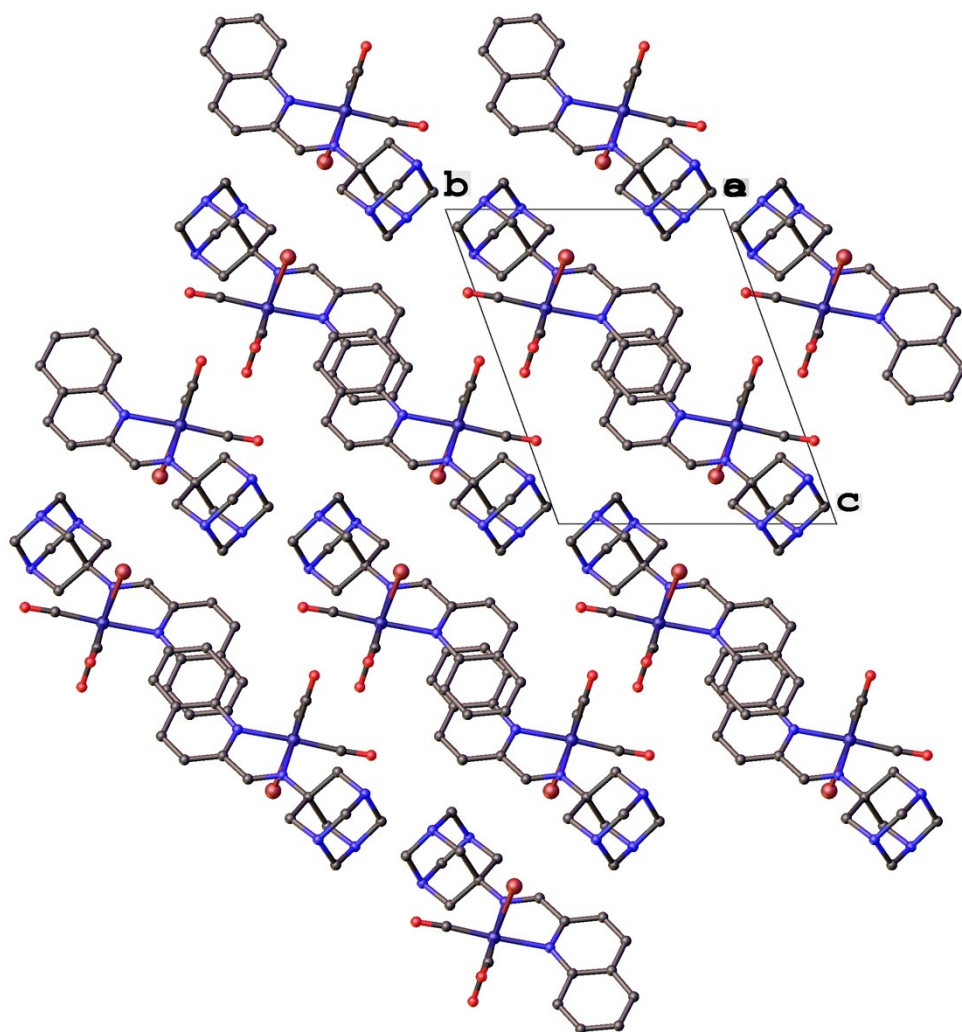


Fig. S3. Packing diagram of **3** along a axis

Determination of Thermodynamic Solubility of 2

15 mg of the complex was placed into 0.5 mL of deionized (DI) water and the solution was allowed to rock overnight in darkness. The solution was then spun down at 16 K g for 5 min to form a pellet of the undissolved solid and the supernatant was carefully pipetted into a separate vessel. 10 μ L of this saturated solution was diluted into 450 μ L of DI water for quantification. A standard series was prepared by fully dissolving 5.5 mg of the complex into 5 mL of DI water and serially diluting (1:1) 5x resulting in solutions that span from 1.1 mg/mL to 0.069 mg/mL. These solutions were quantified using a Thermo NanoDrop 2000c UV-Vis spectrometer. The complex showed strong absorbance at a wavelength of 409 nm that was in the dynamic range of the instrument and as such this wavelength's intensity was monitored for quantification. All measurements were made in triplicate and the average value was used. The resulting standard curve and linear regression were used to determine the concentration of 1:50 dilution of the saturated solution as indicated by the red "X" mark on the curve. This concentration value was then multiplied by 50 to obtain the concentration of the complex in the saturated solution resulting in a value of 13.8 mg/mL.

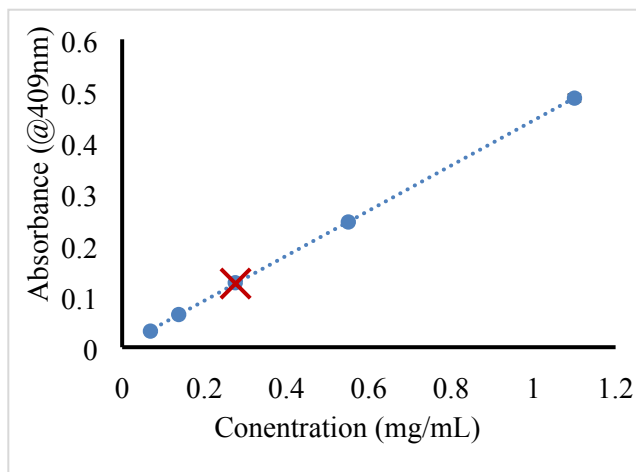


Fig. S4. Standard curve for aqueous solubility determination. 5 blue points represent mean values from 3 replicates of a serial dilution. Error bars representing standard deviation of the replicates are too small to see as plotted. The y value of "X" represents the absorbance of the 1:50 dilution of the saturated solution and the x value is fit from the indicated regression line.

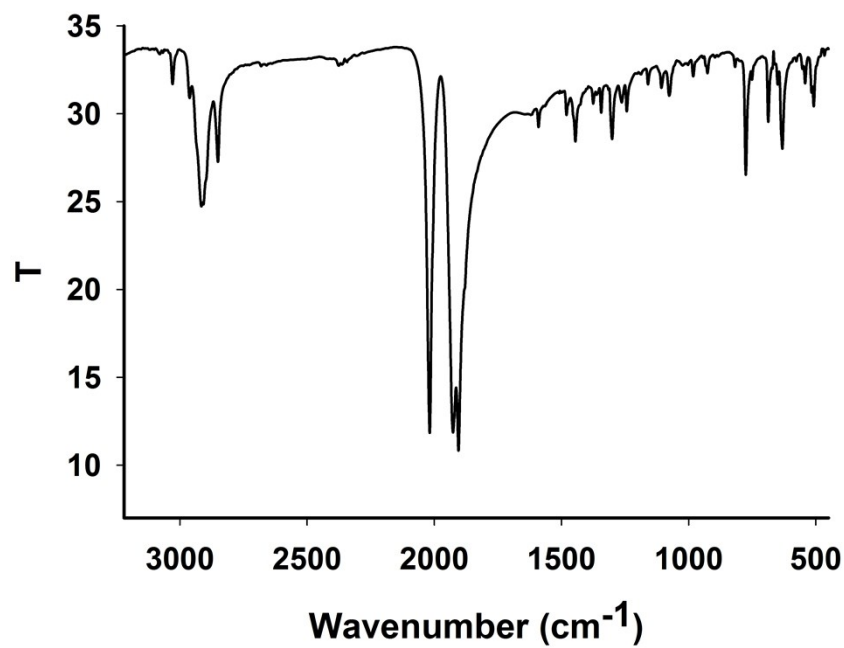


Fig. S5. IR spectrum of complex 1 (KBr pellet)

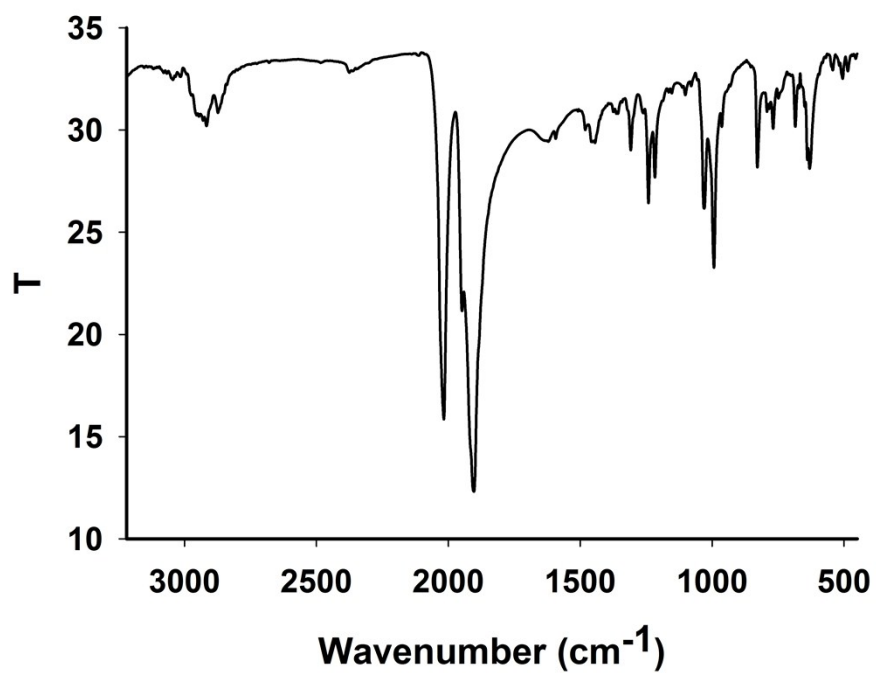


Fig. S6. IR spectrum of complex 2 (KBr pellet)

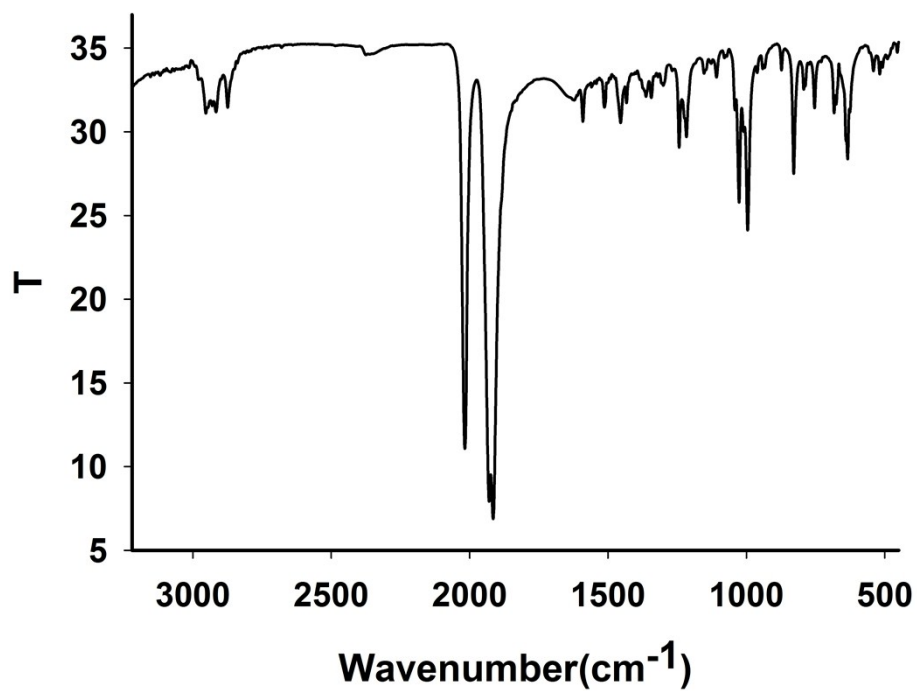


Fig. S7. IR spectrum of complex 3 (KBr pellet)

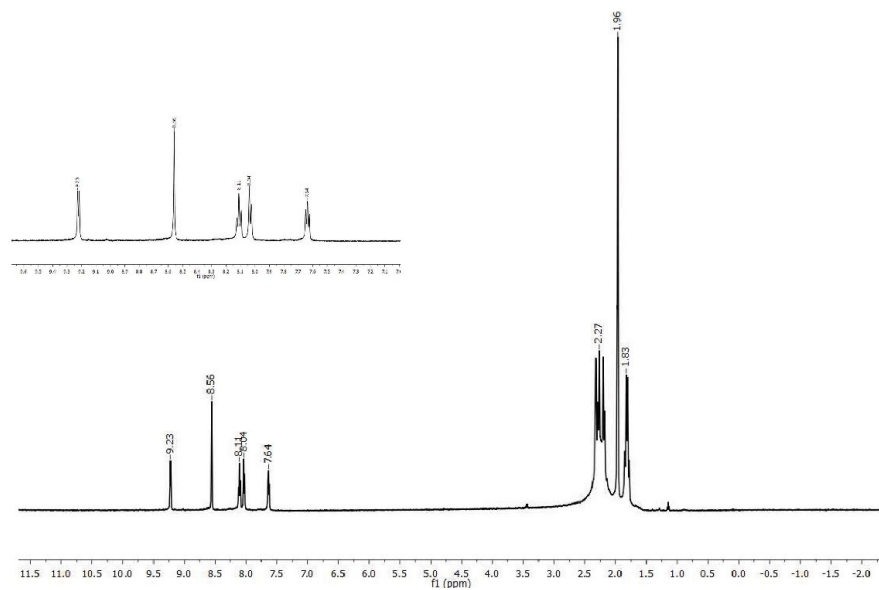


Fig. S8. 500 MHz ¹H NMR spectrum of complex 1 in CD₃CN at 298 K

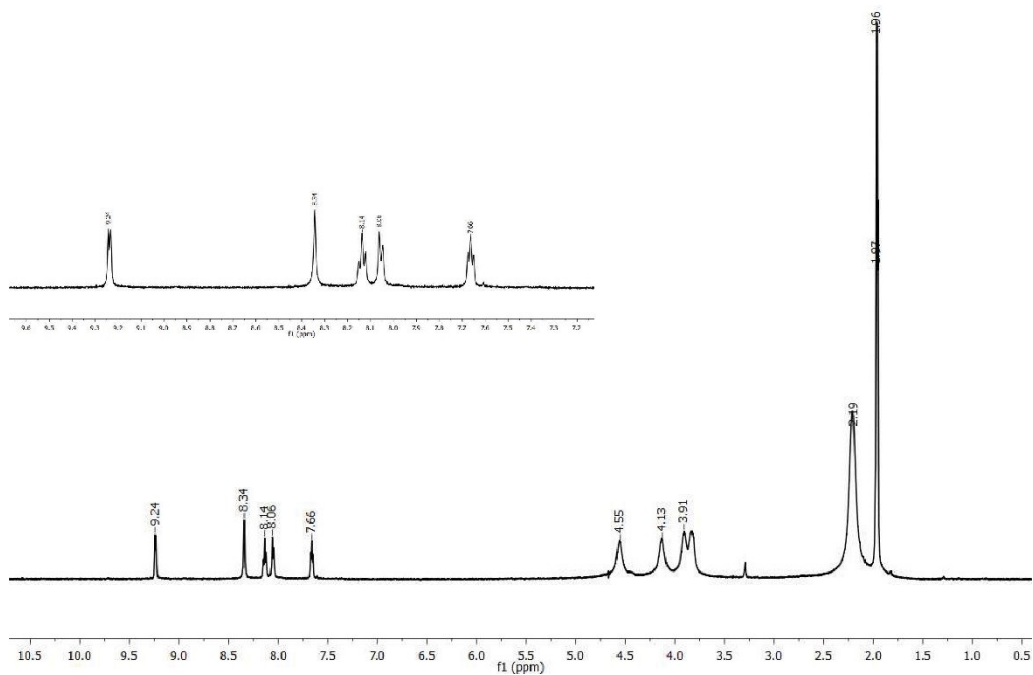


Fig. S9. 500 MHz ^1H NMR spectrum of complex **2** in CD_3CN at 298 K

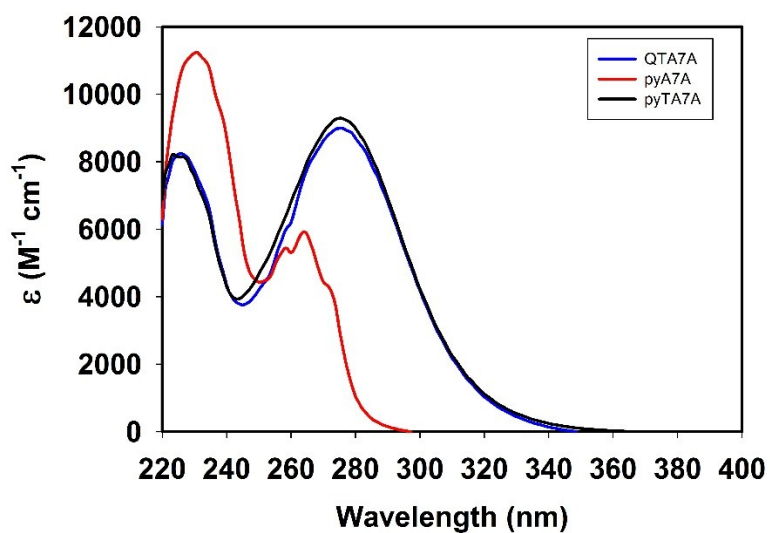


Fig. S10. Electronic absorption spectra of pyAm (red trace), pyTAm (black trace) and qyTAm (blue trace) in CH_2Cl_2 solution at 298 K

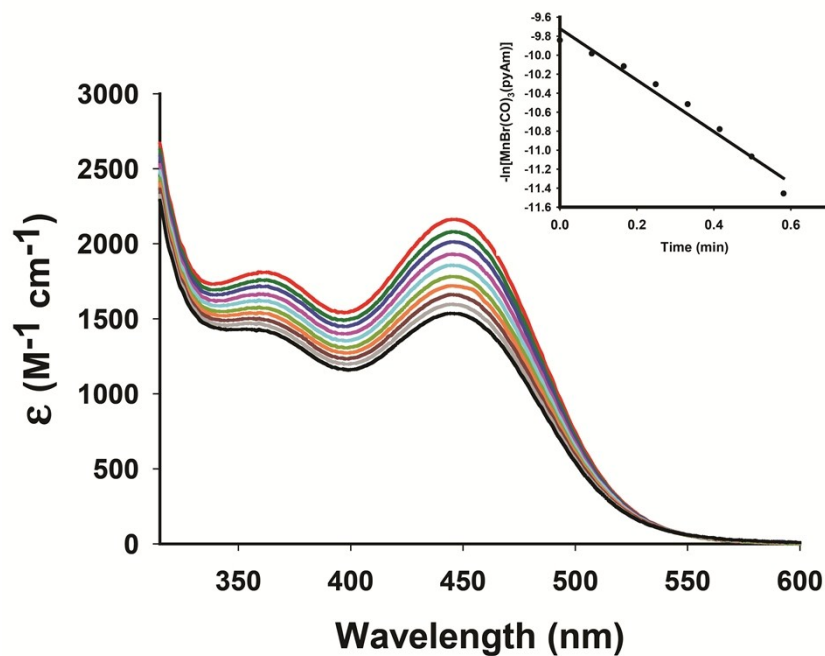


Fig. S11. Changes in the electronic absorption spectrum of complex **1** in CH_2Cl_2 upon exposure to monochromatic visible light with $\lambda = 450 \text{ nm}$ (conc, $1.83 \times 10^{-4} \text{ M}$, power: 1 mW/cm^2). The inset displays the k_{CO} rate plots for complex ($k_{\text{CO}} = 2.71 \text{ min}^{-1}$).

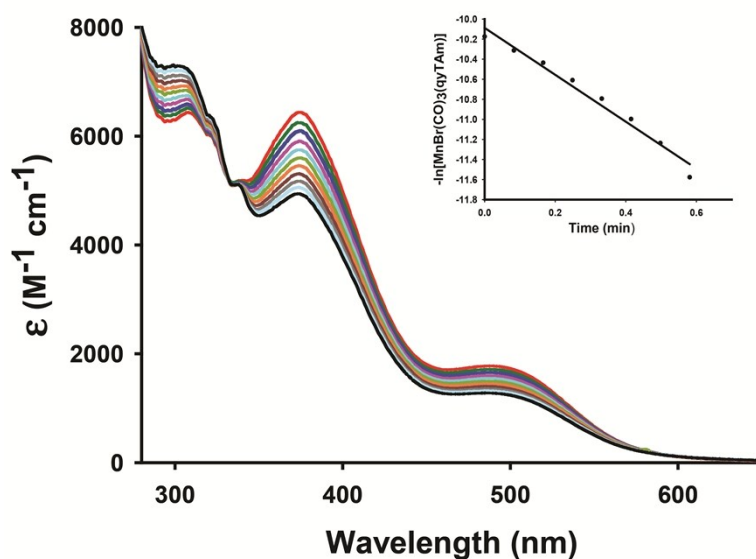


Fig. S12. Changes in the electronic absorption spectrum of complex **3** in CH_2Cl_2 upon exposure to monochromatic visible light with $\lambda = 450 \text{ nm}$ (conc, $1.64 \times 10^{-4} \text{ M}$, power: 1 mW/cm^2). The inset displays the k_{CO} rate plots for complex ($k_{\text{CO}} = 2.34 \text{ min}^{-1}$).

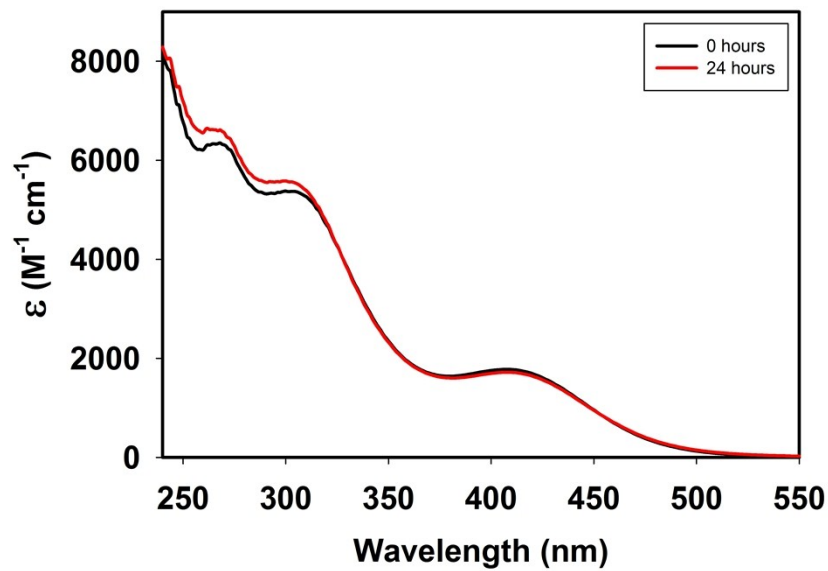


Fig. S13. UV-Vis spectral traces of 2 in PBS at 298 K in presence of glutathione

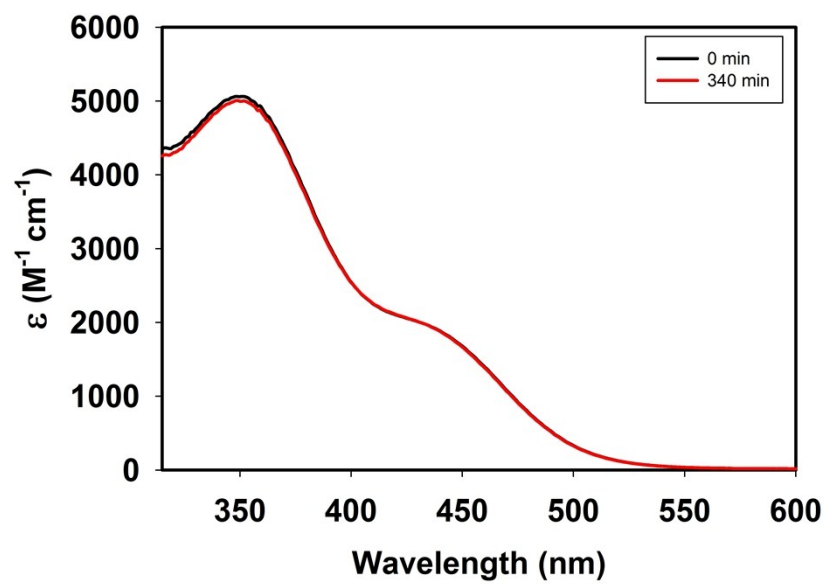


Fig. S14. UV-Vis spectral traces of 2 in DMSO at 298 K

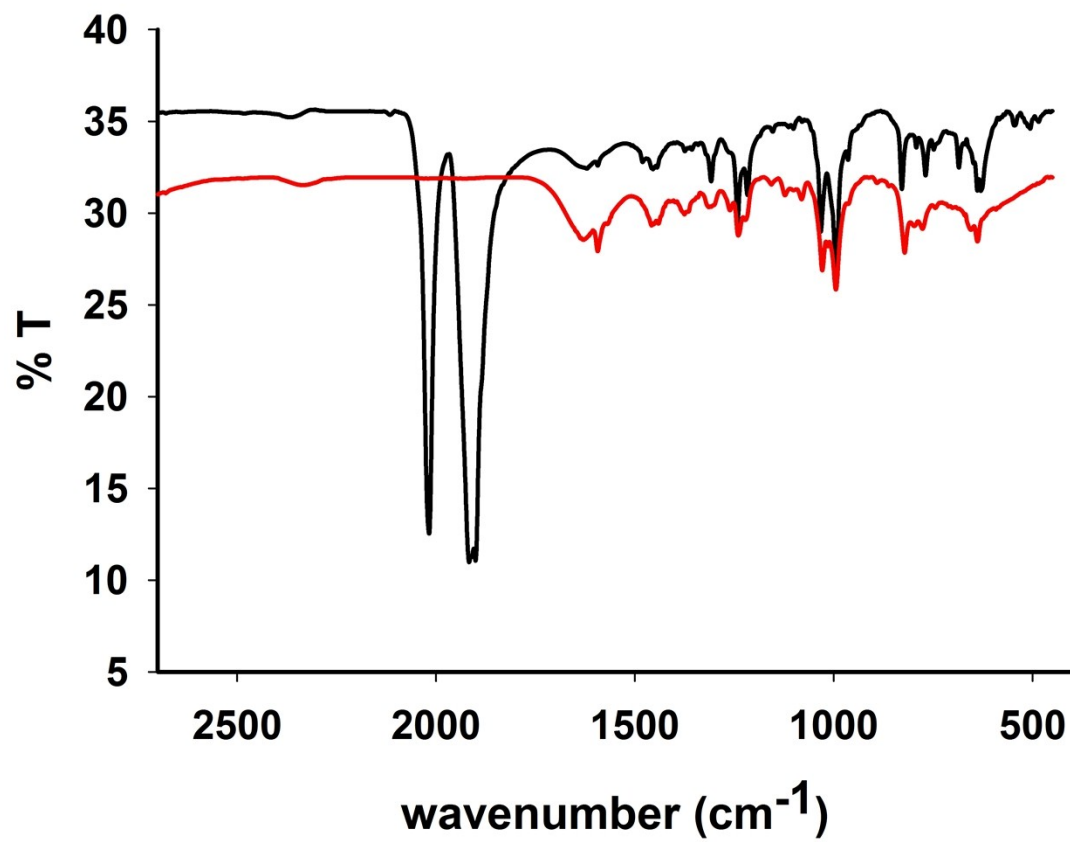


Fig. S15. Infrared spectra of **2** before (black trace) and after (red trace) visible light illumination (KBr disk)

Table S1. Selected bond distances (Å) and angles (°) of **1** and **2** along with optimized DFT bond Distances and bond angles for comparison.

	Complex 1		Complex 2	
	X-ray	DFT	X-ray	DFT
Mn1–C1	1.959(8)	1.775	1.899(5)	1.776
Mn1–C2	1.807(5)	1.788	1.815(4)	1.791
Mn1–C3	1.807(5)	1.794	1.801(4)	1.794
Mn1–N1	2.051(4)	2.033	2.049(3)	2.035
Mn1–N2	2.106(3)	2.104	2.092(3)	2.099
Mn1–Br1	2.5216(9)	2.5209	2.5082(6)	2.5185
C2–Mn1–C3	86.2(2)	87.2	85.16(16)	88.1
C2–Mn1–C1	89.7(3)	92.8	93.70(16)	93.1
C3–Mn1–C1	91.2(2)	92.6	91.12(16)	93.2
C2–Mn1–N1	94.23(19)	93.5	95.94(14)	93.1
C3–Mn1–N1	177.56(18)	174.3	177.03(13)	174.0
C1–Mn1–N1	91.18(19)	93.0	91.57(14)	92.6
C2–Mn1–N2	173.26(19)	171.5	172.44(14)	170.0
C3–Mn1–N2	100.44(17)	99.5	99.83(13)	98.9
C1–Mn1–N2	91.12(18)	92.0	91.88(13)	92.9
N1–Mn1–N2	79.08(13)	79.3	78.80(10)	79.2
C2–Mn1–Br1	91.1(2)	86.5	86.61(12)	85.8
C3–Mn1–Br1	90.43(15)	88.7	91.73(11)	88.5
C1–Mn1–Br1	178.21(16)	178.6	177.15(11)	178.0
N1–Mn1–Br1	87.16(11)	85.8	85.58(8)	85.8
N2–Mn1–Br1	87.89(9)	88.4	87.56(7)	87.9

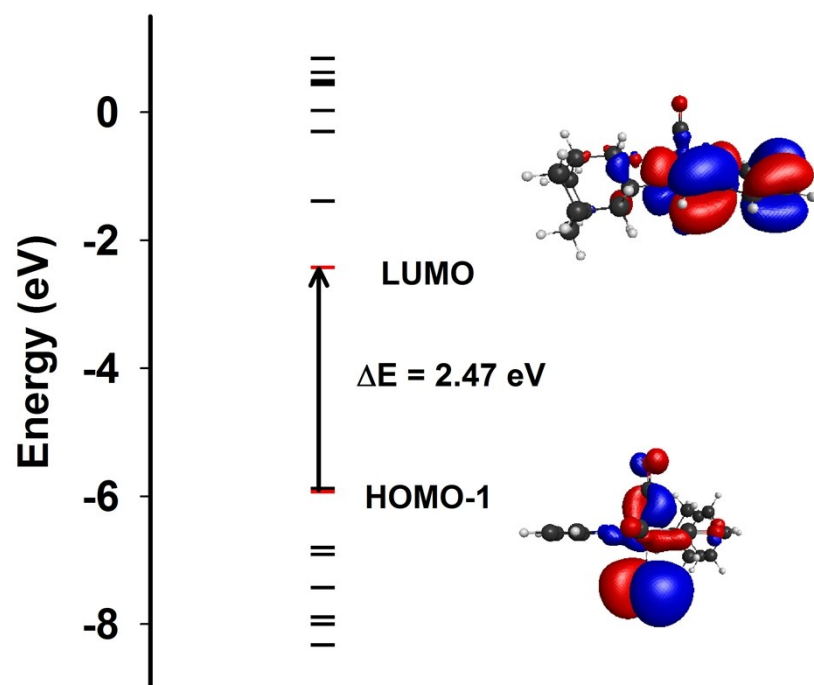


Fig. S16. Calculated energy diagram for **1**. The most prominent MOs involved with transition associated with CO photo release under visible light illumination are shown.